Dynamic autoresonance and global chaos in a slowly evolving system of two coupled oscillators

G. Cohen and B. Meerson

Racah Institute of Physics, Hebrew University of Jerusalem, Jerusalem 91904, Israel

(Received 1 July 1992)

A Hamiltonian system of two coupled oscillators, a linear and a nonlinear, is investigated analytically and numerically in the case when the frequency of the linear oscillator is allowed to vary slowly in time. We focus mainly on the dynamic-autoresonance (DAR) effect, i.e., a persisting phase locking between the two oscillators, accompanied by a large, though slow, energy exchange between them. The two-oscillator model is motivated by the necessity, in some applications, of taking into account the energy depletion of the driving field. The theory of the internal first-order resonances in two-dimensional Hamiltonian systems is generalized to the case of a slow parameter variation. Three constraints for the existence of DAR are found, and the theory is verified numerically. Also, several routes from order to global chaos and from global chaos to order are observed numerically.

I. INTRODUCTION

The model of an oscillator driven by an external force, periodic in time, is ubiquitous in physics. Its elementary version is a linear oscillator with constant parameters acted upon by a sinusoidal driving force. An important generalization of the elementary model involves non-linearity of the oscillator. Another generalization is allowing the parameters of the oscillator and/or the external field to vary slowly with time. Combining these two, we arrive at the model of a nonlinear driven oscillator with slowly varying parameters. This model has numerous applications (see later) and it is not so simple anymore.

The frequency of nonlinear oscillations depends on their amplitude. Therefore the infinite growth of the amplitude, obtained for a linear, dissipation-free oscillator driven by a resonant external force, is not possible for a nonlinear oscillator with constant parameters [1]. However, if the frequency of the driving force is allowed to depend slowly on time, it can be "tapered" in such a way that the resonant growth will continue. If the change in the driving frequency is slow enough, the oscillator will continue to perform nonlinear oscillations around the (time-dependent) resonant value of the action variable. This effect, which is called "dynamic autoresonance" (DAR), or dynamic phase locking, was actually noticed already in the early theory of the synchrotron [2]. Examples of DAR are well known in accelerator physics [3,4] and free-electron lasers [5], where the phenomenon is exploited for particle acceleration and efficiency enhancement, respectively. Recently, DAR has found applications in the plasma-beat-wave acceleration schemes [6,7] and microwave excitation of the Rydberg atoms ("the Rydberg accelerator") [8]. In essence, in the process of DAR a slow drift is superimposed on the relatively fast periodic changes in the amplitude resulting from the "nonlinear" oscillations. Therefore, over a time interval much longer than the period of the nonlinear oscillations,

the oscillator is able to extract a large amount of energy from the driving source.

In all the above-mentioned works related to various applications of DAR, the energy of the external driving force was assumed to be inexhaustable. In some of the schemes mentioned, there are ranges of parameters, for which the finiteness of energy stored in the external field must be taken into account. Examples are provided by the energy depletion of the two laser pulses, exciting an intense plasma wave in the plasma-beat-wave scheme [7], as well as by the energy depletion of the plasma wave itself in the process of particle acceleration [6].

A simple model system possessing the property of energy depletion is provided by two weakly coupled oscillators:

$$\ddot{x}_1 + x_1^3 = \epsilon x_2 , \tag{1a}$$

$$\ddot{x}_2 + \omega^2(t)x_2 = \epsilon x_1 , \tag{1b}$$

where ϵ is a small coupling parameter and $\omega(t)$ is a slow time-dependent frequency.

In the equation of motion (1a) for the nonlinear oscillator, the "driving force" results from the weak coupling to another (in our model, linear) oscillator rather than from an inexhaustable external field. We shall see that the model (1), though quite specific, possesses a number of general properties.

Equations (1a) and (1b) can be obtained from the following Hamiltonian:

$$H = \frac{\dot{x}_1^2 + \dot{x}_2^2}{2} + \frac{x_1^4}{4} + \frac{\omega^2(t)x_2^2}{2} - \epsilon x_1 x_2 . \tag{2}$$

The present paper is devoted to the study of the model (1) and (2). We first consider, in Sec. II, the "static" version of the model (ω independent of t). We start with the single-resonance perturbation theory with respect to ϵ to study the structure of the phase space of the static model, and then verify the theory by numerical calculations.

Also, we use the Chirikov criterion of overlapping resonances [9] to interpret the transition to global chaos, which is seen numerically in the static model. In Sec. III we generalize the perturbation theory to describe slowly evolving two-dimensional Hamiltonian systems in the case of a weak coupling. We find an adiabatic invariant for the motion near resonances, which makes this system integrable for the majority of initial conditions and enables us to describe the DAR effect. Also, we employ the modified (time-dependent) Chirikov criterion [8,10] to predict the *time moment* of the transition to global chaos in the system with varying parameters. The results of Secs. II and III are applied to the system (1) and (2) (the "dynamic" model) in Sec. IV. We formulate and verify numerically three criteria for the existence of DAR. In Sec. V, we briefly describe the development of *explicitly time-dependent* global chaos in the model (1) and (2). Section VI contains a brief summary and conclusions.

II. STATIC MODEL

We are starting with the system (1) with *no* explicit time dependence: $\omega(t) = \omega_0 = $ const. We shall call this model static and rewrite its Hamiltonian (2) as a sum of the unperturbed H_0 and perturbed H_1 parts:

$$H = H_0 + \epsilon H_1 , \tag{3}$$

where

$$H_0 = \frac{\dot{x}_1^2 + \dot{x}_2^2}{2} + \frac{x_1^4}{4} + \frac{\omega_0^2 x_2^2}{2} , \quad H_1 = -x_1 x_2 . \tag{4}$$

For the static model, the total energy is conserved, $H = $ const, while the corresponding equations of motion have the form of Eqs. (1) with $\omega = \omega_0 = $ const.

A. The unperturbed system

We first transform the unperturbed system to the action-angle variables J_1, J_2, θ_1, and θ_2. For the first nonlinear oscillator we obtain [9]

$$J_1 = \tilde{A} E_1^{3/4} , \quad \tilde{A} = \frac{4\sqrt{2}}{3\pi} K(1/\sqrt{2}) . \tag{5}$$

J_1 and E_1 are the action and energy of the first unper-

turbed oscillator, $K(m)$ is the complete elliptic integral of the first kind [11].

Inverting for E_1, we have

$$E_1 = A J_1^{4/3} , \quad A = \tilde{A}^{-4/3} \cong 0.867 . \tag{6}$$

The cyclic frequency of the unperturbed first oscillator is

$$\omega_1 = \frac{\partial H_0}{\partial J_1} = B J_1^{1/3} , \quad B = \frac{4}{3} A \cong 1.156 . \tag{7}$$

For the phase coordinate conjugate to J_1 we have [9]

$$\frac{2K\theta_1}{\pi} = F(\eta, 1/\sqrt{2}) , \quad \eta = \cos^{-1}[x_1/(4E_1)] , \tag{8}$$

where $F(\omega, m)$ is the incomplete elliptic integral of the first kind [11] with modulus m. From now on we shall write K instead of $K(1/\sqrt{2})$. Inverting for x_1, we obtain

$$x_1 = (4E_1)^{1/4} \text{cn} \left[\frac{2K\theta_1}{\pi} \right] , \tag{9}$$

where cn$w$ is one of the Jacobi elliptic functions. Using the Fourier expansion [11] for cn$w$, we can rewrite Eq. (9) in the following form:

$$x_1 = \sqrt{2} D J_1^{1/3} \sum_{n=1}^{\infty} a_{2n-1} \cos[(2n-1)\theta_1] , \tag{10}$$

where

$$\begin{aligned} a_{2n-1} &= \cosh^{-1}[\pi(n-1/2)] , \\ D &= (\sqrt{2}\pi/K)(3\pi/4\sqrt{2}K)^{1/3} \cong 2.312 . \end{aligned} \tag{11}$$

Since $a_{2n-1}/a_{2n+1} \cong 23 \gg 1$, the motion of the first oscillator is almost harmonic, but essentially nonlinear.

For the second linear oscillator we have $x_2 = (2J_2/\omega_0)^{1/2}\cos\theta_2$, where $J_2 = E_2/\omega_0$, J_2 and E_2 are the action and energy of the unperturbed second oscillator, respectively.

B. Perturbed system

Let us write the Hamiltonian (3) of the perturbed system in the action-angle variables:

$$H(\mathbf{J}, \boldsymbol{\theta}) = A J_1^{4/3} + \omega_0 J_2 - \epsilon \frac{D}{\omega_0^{1/2}} J_2^{1/2} J_1^{1/3} \sum_{n=1}^{\infty} a_{2n-1} \{\cos[\theta_2 + (2n-1)\theta_1] + \cos[\theta_2 - (2n-1)\theta_1]\} , \tag{12}$$

where $\mathbf{J} = (J_1, J_2)$, $\boldsymbol{\theta} = (\theta_1, \theta_1)$. If the term proportional to ϵ is treated perturbatively, we find resonances whenever $(2n-1)\omega_1(J_1) = \omega_2 = \omega_0$. The corresponding resonant values of J_1 and E_1 are

$$J_1^r = \frac{\omega_0^3}{B^3(2n-1)^3} , \quad E_1^r = \frac{A}{B^4} \frac{\omega_0^4}{(2n-1)^4} , \tag{13}$$

respectively. It is seen that for energies larger than

$E_{\min} = A\omega_0^4/B^4$ all the resonances can be excited, and that the smaller the n, the higher the energy (and the action) of the corresponding resonance. We assume that $E > E_{\min}$ throughout the paper.

For sufficiently small ϵ and for the majority of initial conditions, we can treat the problem perturbatively [12] and study the motion in the vicinity of (isolated) resonances. The resonant part of the Hamiltonian of the static model can be written as

$$H^{\prime} = \langle \hat{H}(\hat{\mathbf{J}}, \hat{\boldsymbol{\theta}}) \rangle_{\hat{\theta}_2}$$

$$= A[(2n-1)\hat{J}_1]^{4/3} + \omega_0(\hat{J}_2 - \hat{J}_1)$$

$$- \epsilon \frac{Da_{2n-1}}{\omega_0^{1/2}} (\hat{J}_2 - \hat{J}_1)^{1/2} [(2n-1)\hat{J}_1]^{1/3} \cos\hat{\theta}_1 \, ,$$

$$(14)$$

where new variables have been introduced:

$$\hat{J}_1 = \frac{1}{(2n-1)} J_1, \quad \hat{J}_2 = J_2 + \frac{1}{(2n-1)} J_1 \, , \qquad (15)$$

$$\hat{\theta}_1 = (2n-1)\theta_1 - \theta_2, \quad \hat{\theta}_2 = \theta_2 \, . \qquad (16)$$

Since the phase $\hat{\theta}_2$ has become cyclic, $\hat{J}_2 = \text{const} = C_n$. This well-known integral of motion [12] makes the system integrable for small ϵ [13].

Now we calculate $C_n - \hat{J}_1$, entering the interaction term in (14), in the zeroth order in ϵ (which is sufficient for obtaining the "nonlinear frequency" and the width of the resonant oscillations, see below, in the first order in $\epsilon^{1/2}$). Omitting the subscript 1 in $\hat{J}_1$ and $\hat{\theta}_1$, we have

$$C_n^0 - \hat{J}^0 = \frac{E_2^0}{\omega_0} = \frac{E^0 - E_1^0}{\omega_0} - \frac{E - \dfrac{A}{B^4}\dfrac{\omega_0^4}{(2n-1)^4}}{\omega_0}$$

$$\equiv \frac{L_n(E, \omega_0)}{\omega_0} \, , \qquad (17)$$

where we have written $E^0 = E$, which means that we do not put any energy in the coupling term at $t = 0$. The inequality $E > E_{\min}$ implies that $L_n(E, \omega_0) > 0$.

The location of the fixed points of the Hamiltonian (14) is given, in the zero order in ϵ, by Eq. (13) for J_1. On the surface of section (x_1, p_1), defined by conditions $x_2 = 0$ and $p_2 > 0$, we have

$$\theta_1 = \frac{2\pi k + \pi/2}{(2n-1)}, \quad \theta_1 = \frac{2\pi k - \pi/2}{(2n-1)} \qquad (18)$$

for the stable and unstable fixed points, respectively.

Two important characteristics of the motion inside the islands are the nonlinear period

$$T \cong 9.8 \frac{23^{(n-1)/2} \omega_0}{(2n-1)^{3/2} L_n^{1/4}(E, \omega_0)} \epsilon^{-1/2} \, , \qquad (19)$$

estimated for the trajectories close to the stable fixed point, and the resonance width (the maximum excursion of the particles in the resonance):

$$\frac{\Delta J_{1\max}}{J_1^{\prime}} = \frac{\Delta \hat{J}_{\max}}{\hat{J}^{\prime}} \cong 7.69 \frac{(2n-1)^{3/2} L_n^{1/4}(E, \omega_0)}{23^{(n-1)/2} \omega_0^2} \epsilon^{1/2} \, .$$

$$(20)$$

Figure 1 shows an example of the surface of section (x_1, p_1) for $E = 169$, $\epsilon = 0.03$, and $\omega(t) = \omega_0 = 4$, obtained numerically. The location of the fixed points coincides with the theoretical prediction. Also, our estimates of $\Delta \hat{J}_{\max}/\hat{J}$ and the nonlinear period agree well with the corresponding values obtained numerically for small ϵ.

Now we apply the Chirikov criterion [9] of overlapping of the first-order resonances to estimate the critical value of ϵ for the transition to global chaos:

$$\frac{|\hat{J}_{1n}^{\prime} - \hat{J}_{1n+1}^{\prime}|}{\frac{1}{2}[\Delta \hat{J}_{1n} + \Delta \hat{J}_{1n+1}]} = 1 \, , \qquad (21)$$

where $\hat{J}_{1n}^{\prime}$ and $\hat{J}_{1n+1}^{\prime}$ denote the resonant values of $\hat{J}_1$ for two neighboring resonances, while $\Delta \hat{J}_{1n}$ and $\Delta \hat{J}_{1n+1}$ denote the islands' widths, given by Eq. (20). Using Eqs. (13) and (20), we rewrite criterion (21) in the following form:

$$\epsilon_{\text{ch}} \cong 0.067 \frac{\omega_0^4 (24n^2 + 2)^2 23^n}{(4n^2 - 1)^3}$$

$$\times [23^{1/2}(2n+1)^{3/2} L_n^{1/4}(E, \omega_0)$$

$$+ (2n-1)^{3/2} L_{n+1}^{1/4}(E, \omega_0)]^{-2} \, . \qquad (22)$$

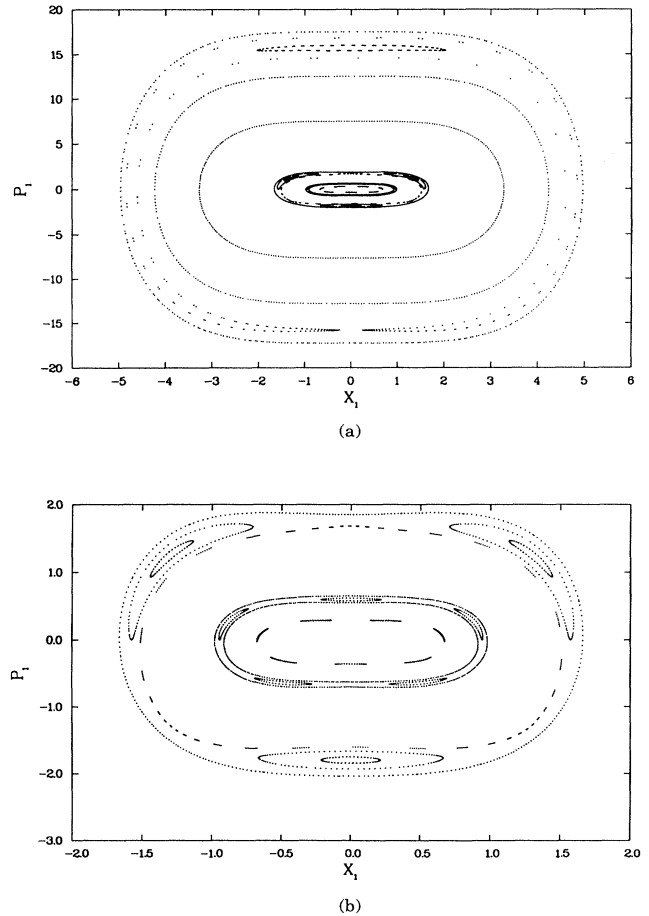Figure 2 shows ϵ_{ch} predicted by Eq. (22), as a function

(a)

(b)

FIG. 1. The (x_1, p_1) surface of section for $E = 169$, $\omega_0 = 4$, and $\epsilon = 0.03$. (a) All the resonances up to $n = 4$ are shown, the $n = 1$ resonance being the outer one. (b) Enlargement of the central region. The resonances corresponding to higher values of n are clearly seen.
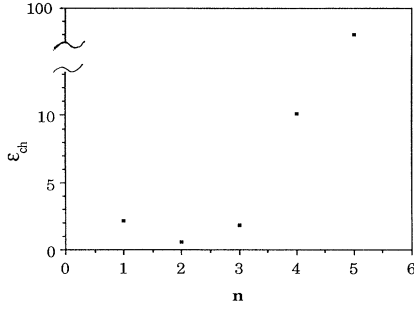
FIG. 2. ϵ_{ch} for different resonances (values of n), as predicted by the Chirikov criterion for the transition to global chaos for our system [Eq. (22)]. $E = 169$ and $\omega_0 = 4$.

of the number of resonance n. We see that the most unstable resonance is $n = 2$, while for $n > 3$ ϵ_{ch} grows with n very fast. We shall concentrate in this work on the regions of the surface of section where the resonances $n = 1, 2,$ and 3 are important.

Figures 3–5 show the same surface of section for increasing values of ϵ. Up to $\epsilon = 0.8$, global chaos exists only in the region of $n = 2$, as predicted by Eq. (20). For $n = 2$, the value of ϵ for which the last Kolmogorov-Arnold-Moser curve is destroyed is found to be $\varepsilon = 0.65$, which is quite a good agreement with Eq. (22).

III. SLOWLY EVOLVING HAMILTONIANS

Let us consider a slowly evolving, weakly perturbed Hamiltonian

$$H = H_0(\mathbf{x}, \mathbf{p}, t) + \epsilon H_1(\mathbf{x}, \mathbf{p}, t) , \tag{23}$$

where H_0 describes a system which *was* integrable when there was *no* explicit time dependence in it, and H_1 denotes a small "nonintegrable" perturbation.

For a general time dependence in H_0, there is no canonical transformation, which would enable us to write the first term in the form $H_0(\mathbf{J}, t)$. However, if this time
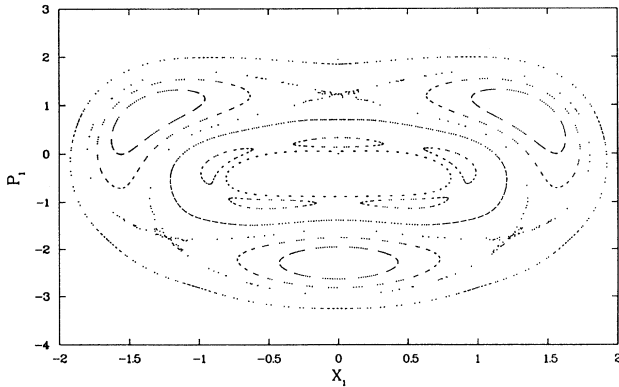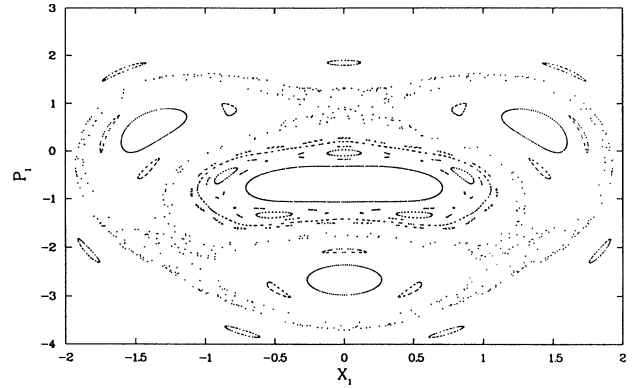

FIG. 4. The system en route to chaos. The central region of the (x_1, p_1) surface of section for $E = 169$, $\omega_0 = 4$, and $\epsilon = 0.6$. Secondary islands and stochastic layers are clearly seen.

dependence is sufficiently slow, J_1 and J_2 become adiabatic invariants [1], the part H_0 integrable and Eq. (23) can be rewritten as

$$H = H_0(\mathbf{J}, t) + \epsilon H_1(\mathbf{J}, \boldsymbol{\theta}, t) , \tag{24}$$

where H_1 is still a periodic function of θ_1 and θ_2. The unperturbed frequencies are now slowly time dependent. Therefore, treating ϵH_1 as a perturbation, we arrive at the same first-order resonances as before, but the resonance conditions $\omega_2(J_2)/\omega_1(J_1) = r/s$ now become slowly time dependent. In other words, the phase locking between the two oscillators can be preserved despite the changes in the oscillator parameters, which can lead to the corresponding (and possibly large) changes in the frequencies ω_1 and ω_2.

Similarly to the time-independent case, we canonically transform the Hamiltonian to the new variables $\hat{\mathbf{J}}, \hat{\boldsymbol{\theta}}$ in order to describe the motion in the vicinity of an isolated resonance. Since the corresponding generating function

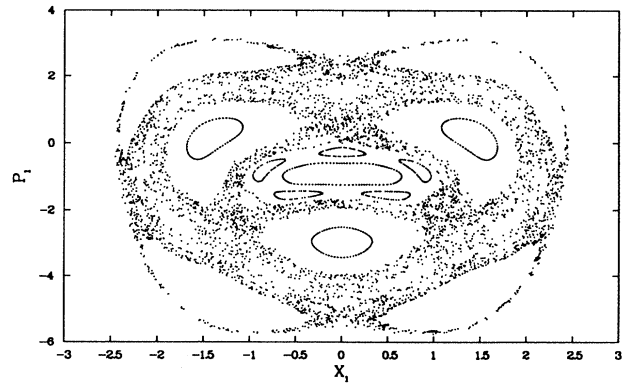$$F = (r\theta_1 - s\theta_2)\hat{J}_1 + \theta_2\hat{J}_2 \tag{25}$$

FIG. 3. The central region of the (x_1, p_1) surface of section for $E = 169$, $\omega_0 = 4$, and $\epsilon = 0.36$. The stochastic layer in the vicinity of the $n = 2$ separatrix is seen.

FIG. 5. Global chaos in the system. The (x_1, p_1) surface of section for $E = 169$, $\omega_0 = 4$, and $\epsilon = 0.8$. The chaotic region is generated from a single trajectory.

has no explicit time dependence, the results obtained for the time-independent case remain valid, but with the explicit slow time dependence inserted into them. Averaging over $\hat{\theta}_2$, we obtain in first order in ϵ

$$H^{\sim}(t) = H_0^{\sim}(\hat{\mathbf{J}}, t) + \epsilon H_1^{\sim}(\hat{\mathbf{J}}, \hat{\theta}_1, t) , \tag{26}$$

where

$$H_0^{\sim}(t) = \hat{H}_0(\hat{\mathbf{J}}, t) \tag{27}$$

and

$$H_1^{\sim}(t) = \langle \hat{H}_1(\hat{\mathbf{J}}, \hat{\theta}, t) \rangle_{\hat{\theta}_2} = \sum_{p=0}^{\infty} H_{-pr, ps}(\hat{\mathbf{J}}, t) \exp[-ip\hat{\theta}_1] . \tag{28}$$

Here $\hat{J}_2$ is again an integral of motion, which generalizes the similar integral for time-independent systems. However, in addition to the smallness of ϵ, it requires now the slowness of the explicit time dependence of the Hamiltonian. Therefore the motion becomes effectively a motion of a system with a single degree of freedom, slowly dependent on time. The slowness of the time dependence leads for the majority of initial conditions, to the existence of an adiabatic invariant of the system, i.e., to integrability. The exact criterion for the slowness of the explicit time dependence is not easy to obtain. However, it is clear that the characteristic time scale of the explicit time dependence must be very large compared to the (slowly time-dependent) characteristic nonlinear time scale of the system (that is the nonlinear period of the oscillations around the resonance; see below).

Limiting ourselves to the Fourier components $p - 0, 1$, and -1 (that is, assuming that the higher components fall sufficiently rapidly with p, as is normally the case [12]), we arrive at the following expression:

$$H^{\sim}(t) = \hat{H}_0(\hat{\mathbf{J}}, t) + \epsilon H_{0,0}(\hat{\mathbf{J}}, t) + 2\epsilon H_{r,-s}(\hat{\mathbf{J}}, t)\cos\hat{\theta}_1 , \tag{29}$$

where we have assumed, without any loss of generality, that the Fourier coefficients are real. Now we can use the "pendulum approximation" [9,12] for the motion in the vicinity of the resonances with the slowly time-dependent values plugged into the equations. The nonlinear frequency of the oscillations becomes

$$\hat{v}(t) \equiv \hat{\omega}_1(t) = [F(t)G(t)]^{1/2} \frac{\pi}{2K(\kappa)} , \tag{30}$$

while the maximum excursion in the value of the action is

$$\Delta\hat{J}_{1\,\mathrm{max}} = 2\left[\frac{F(t)}{G(t)}\right]^{1/2} , \tag{31}$$

where

$$G(\hat{\mathbf{J}}^{\sim}, t) = \frac{\partial^2 \hat{H}_0}{\partial \hat{J}_1^{\sim 2}} \tag{32}$$

and

$$F(\hat{\mathbf{J}}^{\sim}, t) = -2\epsilon H_{r,-s}(\hat{\mathbf{J}}^{\sim}, t) . \tag{33}$$

The superscript $\sim$ denotes the value of $\mathbf{J}$ at resonance.

The resonance widths now become slowly time dependent. In the case that they increase in time, the resonances can eventually overlap, which gives us an estimate for the *time moment* of transition to global chaos in the system [8,10]. This *time-dependent* Chirikov criterion takes the form of Eq. (21), but with the explicit time dependence added:

$$\frac{|\hat{J}_{1n}^{\sim}(t) - \hat{J}_{1n+1}^{\sim}(t)|}{\frac{1}{2}[\Delta\hat{J}_{1n}(t) + \Delta\hat{J}_{1n+1}(t)]} = 1 . \tag{34}$$

IV. "DYNAMIC" MODEL: DAR, CONSTRAINTS, AND ORDER-CHAOS TRANSITIONS

Now we apply the results of the preceding section to our specific model of two coupled oscillators, described by the Hamiltonian (2). The first-order resonance condition becomes

$$(2n-1)\omega_1 = \omega_2 = \omega(t), \quad \frac{\omega(t)}{\omega_1} = \frac{(2n-1)}{1} , \tag{35}$$

while the corresponding time-dependent value of the action [see Eq. (13)] is

$$J_1^{\sim}(t) = J_1^{\sim}(\omega_1^{\sim}(t)) = \frac{\omega(t)^3}{B^3(2n-1)^3} . \tag{36}$$

We assume the characteristic time of the change in $\omega(t)$ being much larger then the typical nonlinear period of the resonant oscillations (we call this criterion the first constraint on DAR) and look at trajectories in the vicinity of the first-order resonances. Then we can apply Eqs. (26)–(28):

$$\begin{aligned} H^{\sim}(t) &= \langle \hat{H}(\mathbf{J}, \theta, t) \rangle_{\theta_2} \\ &= A[(2n-1)\hat{J}_1(t)]^{4/3} + \omega(t)[\hat{J}_2(t) - \hat{J}_1(t)] \\ &\quad - \epsilon \frac{Da_{2n-1}}{\omega^{1/2}(t)}[\hat{J}_2(t) - \hat{J}_1(t)]^{1/2} \\ &\quad \times [(2n-1)\hat{J}_1(t)]^{1/3}\cos\hat{\theta}_1 , \end{aligned} \tag{37}$$

where $\omega(t)$ has been considered as constant when averaging over $\hat{\theta}_2$.

For the integral of motion $\hat{J}_2$ we obtain

$$\hat{J}_2 = J_2(t) + \frac{1}{(2n-1)}J_1(t) = \mathrm{const} = C_n . \tag{38}$$

We calculate C_n to zero order in ϵ, using the resonant values of J_1 and J_2 [which is equivalent to averaging over the nonlinear period; see Eq. (28)]. Therefore we can write

$$\bar{J}_2(t) + \frac{1}{(2n-1)}\bar{J}_1(t) = C_n \tag{39}$$

where

$$\bar{J}_i(t) = \langle J_i(t) \rangle_{\hat{\theta}_1} , \tag{40}$$

while for C_n we have

$$C_n = \omega^3(0) \left[\frac{E(0)}{\omega^4(0)} + \frac{0.162}{(2n-1)^4} \right] , \qquad (41)$$

where $E(0)$ is the energy of the system at $t = 0$.

Now, if we start a trajectory "trapped" in the island, and change slowly the frequency $\omega(t)$, the system will remain in the resonance and Eq. (34) will hold for $\bar{J}_1$. Under these conditions, the first integral (39) describes the slow drift of the action variables J_1 and J_2, which can lead to significant changes in the values of the actions. Then, using Eq. (5), we see that by slowly increasing $\omega(t)$ we can continuously increase $\bar{E}_1$ via the process of DAR. Note that no special dependence of ω on t is needed to achieve the DAR regime. Figure 6 gives a numerical example of DAR in this model. Shown is J_1, on the surface of section, as a function of time. We chose for $\omega(t)$ the simplest dependence $\omega(t) = \omega_0(1 + \alpha t)$ with a small positive α. In this example, an increase of more than three orders of magnitude in the value of J_1 is achieved.

Equations (39) and (41) make it possible to draw the plot of the drift motion of the system, i.e., motion on the $(\bar{J}_1, \bar{J}_2)$ plane. Neither $\bar{J}_1$ nor $\bar{J}_2$ can be negative, therefore, the integral (39) must break down when either of the actions approaches zero and the corresponding oscillator is depleted of its energy. The energy depletion presents the second constraint on the existence of DAR. The third constraint is related to the region in the $(\bar{J}_1, \bar{J}_2)$ plane where global chaos develops. In order to roughly evaluate the form of the boundary of this region, we can use Eq. (34) and express $\bar{J}_2$, for a fixed value of ϵ, as a function of $\bar{J}_1$. Putting $\bar{J}_{2n}(t) = \bar{J}_{2n+1}(t)$ (which is quite a good approximation for $n > 1$), we obtain

$$\bar{J}_{2n}(t) = [\bar{J}_{1n}(t)]^{7/3} \frac{F_n}{\epsilon^2} , \qquad (42)$$

where

$$F_n \cong \frac{\left\{ 1 - \left[1 + \frac{24n^2}{(2n-1)^3} \right]^{-1} \right\}^4 23^{2n}(2n-1)}{78.8 \left\{ 4.8 + \left[1 + \frac{24n^2}{(2n-1)^3} \right]^{-1/2} \right\}^4} \qquad (43)$$
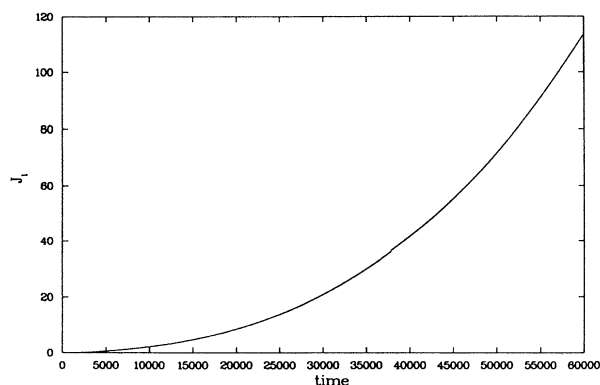

FIG. 6. DAR in the system. Shown is J_1 on the surface of section vs time for $\alpha = 10^{-4}$.

is a positive, n-dependent parameter.

Equation (42) defines a curve in the $(\bar{J}_1, \bar{J}_2)$ plane for which the time-independent Chirikov criterion predicts transition to global chaos in our model. Combining Eqs. (39) and (42), we estimate the position of the intersection point of the curve, describing the motion in the $(\bar{J}_1, \bar{J}_2)$ plane in the regime of DAR, with the boundary of the globally chaotic region. Note that, for a fixed n, the intersection point moves with an increase of ϵ towards higher values of $\bar{J}_1$.

One can think about different possible scenarios of the motion in the $(\bar{J}_1, \bar{J}_2)$ plane, when DAR is sustained for a sufficiently long time and leads to a considerable change in the actions $\bar{J}_1$ and $\bar{J}_2$. Three such scenarios are plotted in Fig. 7. Figure 7(a) shows a trajectory, trapped in the vicinity of a resonance in the "regular" region of the $(\bar{J}_1, \bar{J}_2)$ plane. If $\omega(t)$ is a monotonusly increasing function of time, and the frequency variation is slow enough, the trajectory remains in resonance (DAR regime) until all the energy of the second oscillator is exhausted. Figure 7(b) shows another trajectory that begins in DAR. This time, however, $\omega(t)$ is a monotonously decreasing function of time. In this case the resonance condition breaks down when the trajectory enters the chaotic regime, and it is the first oscillator which loses its energy, but not all of it. Finally, Fig. 7(c) shows a trajectory that begins in the chaotic regime and, because of the increase of $\omega(t)$, passes from the chaotic regime into a DAR trajectory. From there on, the trajectory follows the route
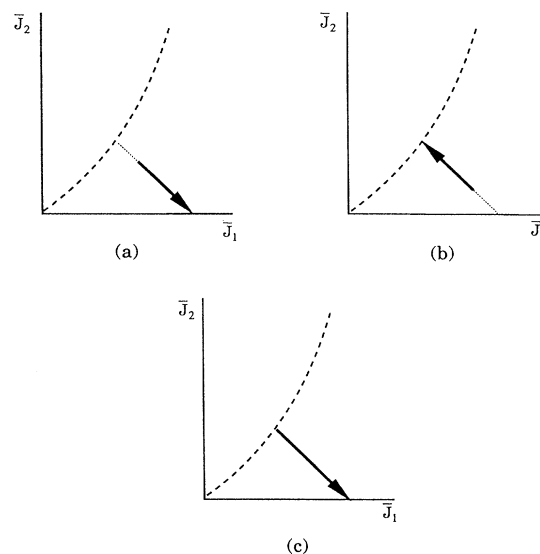

(a)   (b)

(c)

FIG. 7. Schematics of different scenarios for the motion in the $(\bar{J}_1, \bar{J}_2)$ plane. The dotted line represents the integral of motion, Eq. (39), for fixed n. The dashed line represents the solution of Eq. (42) (transition to global chaos) for fixed ϵ and n. The bold lines represent the actual motion in the corresponding scenarios. (a) Energy depletion of the second oscillator. (b) A trajectory changing from DAR to chaos. (c) A trajectory which exists from chaos to DAR.

similar to that shown in Fig. 7(a).

Let us return to the first (adiabaticity) constraint and define the time scale of the nonlinear oscillations as $1/\nu(t)$ and the time scale of the change in $\omega(t)$ as $\omega(t)/\dot{\omega}(t)$. Then, we can loosely write the first constraint as

$$\frac{T_{nl}}{T_{change}} = G_n \left[C_n - \frac{\omega^3(t)}{(2n-1)^4 B^3} \right]^{-1/4} \frac{|\dot{\omega}(t)|}{\epsilon^{1/2}} \ll 1 \ , \quad (44)$$

where

$$G_n \simeq 2 \frac{2K(\kappa)23^{(n-1)/2}}{\pi(2n-1)^{3/2}} \ . \quad (45)$$

It is seen from (44) that, for a prescribed $\omega(t)$, the adiabaticity constraint requires sufficiently large ϵ.

An example where the first constraint breaks before the second oscillator is depleted of its energy, is shown in Fig. 8. The same dependence as before, $\omega(t)=\omega_0(1+\alpha t)$, was chosen, but with a larger α. We see that the system is locked in DAR until the resonance terminates and $\bar{J}_1$ remains constant from there on. Before this point is reached, the *monotonous* increase in the value of $\bar{J}_1$ occurs. Besides, small oscillations in the value of J_1 [the "nonlinear" oscillations averaged over by Eq. (40)] are clearly seen. Finally, when the system leaves DAR, the only oscillations remaining in the value of J_1 (after a relatively short transition period) are the very small, nonresonant oscillations, also seen in Fig. 8. We found that the time-dependent values of the period of the nonlinear oscillations agree well with the prediction of the theory. Also, we checked that, for too large an α, the system always detunes from resonance and enters a nonresonant trajectory, on which it remains forever. For the prescribed linear frequency dependence and given initial conditions, there is a maximum value of α for which DAR regime still exists. We found this maximum to depend strongly on the initial conditions, the typical values varying between 10^{-2} and 10^{-4} (for the chosen parameters $E=169$ and $\omega_0=4$).

We compared the behavior of systems differing from each other in the value of the parameter ϵ *alone*. For this
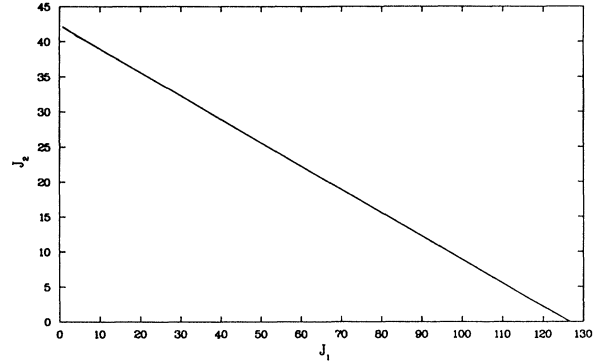
FIG. 9. Energy depletion of the second oscillator. Shown is a trajectory on the (J_1,J_2) plane for $\alpha=10^{-3}$.

purpose we had to choose trajectories corresponding to similar initial conditions. For a given value of α, the time at which each of the trajectories exists from DAR was found. For these times, we calculated the right-hand side of Eq. (44) multiplied by $\epsilon^{1/2}$ for each of the trajectories. The values obtained were found to agree within 50%, which is fairly good taking into account the strong dependence on the initial conditions.

We checked numerically the integral of motion (39) and whether the second constraint on DAR, namely, the depletion of energy of the second oscillator, can be seen. Figure 9 shows a trajectory on the (J_1,J_2) plane close to the resonance $n=2$, computed numerically for $\alpha=10^{-3}$. An increase of two orders of magnitude in the value of J_1 is observed, and the linear dependence between the two actions, predicted by Eq. (39), is clearly seen. The values of C_n obtained numerically agree to within 2% with the values given by Eq. (41). Calculations for different n showed that the values of the slopes of the straight lines obtained numerically coincide with the theoretical prediction, $-1(2n-1)$, with an accuracy of 6%. Also, the second constraint predicts that as $\bar{J}_2$ approaches zero, DAR must terminate. We found numerically (for orbits not far from the stable fixed point) that the time moments at which DAR terminates are not smaller than $0.8t_0$ and never exceed t_0, where t_0 is the time moment for which $\bar{J}_2$ goes to zero according to the theory.

We verified that the second scenario [transition of DAR trajectories to the chaotic regime; Fig. 7(b)] is realized in the system. For this scenario to occur, α must be negative. Figure 10 shows a three-dimensional plot in the (J_1,J_2,t) space for $\alpha=-10^{-4}$. Shown is a trajectory that starts in the DAR regime and later exhibits chaotic wandering in the values of the actions. The numerical values of $\bar{J}_1$ at which the trajectories become chaotic were found to be smaller by a factor of up to 2 than those predicted by the (time-dependent) Chirikov criterion (34). It means that the DAR trajectories go farther than the point at which the Chirikov criterion predicts their entering chaos. This deviation is understandable since the "deeply trapped" trajectories are not destroyed when the resonances have just overlapped.
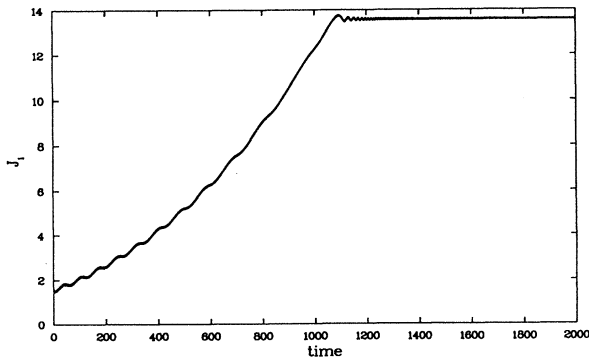
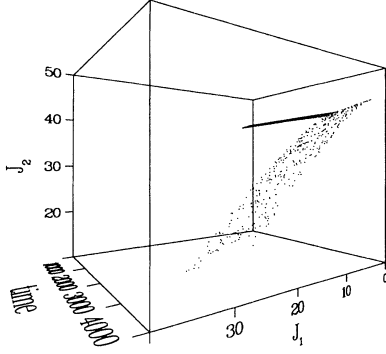The time-dependent Chirikov criterion for the model,

FIG. 8. Demonstration of DAR followed by detuning. Shown is J_1, on the surface of section, as a function of time. $\alpha=10^{-3}$.

FIG. 10. Transition from DAR into chaotic motion. A three-dimensional plot (J_1, J_2, t) for $\alpha = -10^{-4}$.

FIG. 11. Transition from DAR into chaos via a bifurcation. A three-dimensional plot (J_1, J_2, t) for $\alpha = 5 \times 10^{-5}$.

Eq. (34), can be written as

$$\epsilon_{ch} \cong 0.067 \frac{(24n^2 + 2)^2 23^2}{(4n^2 - 1)^3} \omega(t)^{7/2}$$

$$\times [23^{1/4}(2n + 1)^{3/2}(J_{2n})^{1/4}$$

$$+ (2n - 1)^{3/2}(J_{2n+1})^{1/4}]^{-2} . \qquad (46)$$

It is seen from Eq. (46) that we can expect the system to become "more regular" with an increase of $\omega(t)$. Physically it is clear because, for higher values of $\omega(t)$, the second oscillator becomes relatively more energetic and less sensitive to the coupling. For DAR trajectories, this effect is enhanced by an additional dependence of ϵ_{ch} on $\omega(t)$ through $\bar{J}_2$: for an increasing (decreasing) $\omega(t)$, $\bar{J}_2$ grows (decreases) accordingly.

We observed a single mechanism by which "trapped" trajectories entered time-dependent chaos: the bifurcation route, first studied for a one-dimensional kicked rotor with slowly varying kicks [10]. Shown in Fig. 11 is a DAR trajectory, bifurcating to a chain of secondary islands and later to chaos. It is seen that DAR continues inside a secondary island, until the trajectory becomes chaotic.

As for the opposite process, i.e., exit from the time-dependent chaos, we observed three variations of the bifurcation route: (i) the transition from chaos into DAR on a primary island trajectory. This scenario is shown in Fig. 7(c); (ii) the transition from chaos into DAR on a secondary island trajectory, which later on bifurcates to DAR on a primary island trajectory. This is the "mirror" case of the order-chaos transition route presented in Fig. 11; (iii) the exit from chaos into DAR on a secondary island which later terminates on a regular, nonresonant trajectory.

V. SUMMARY

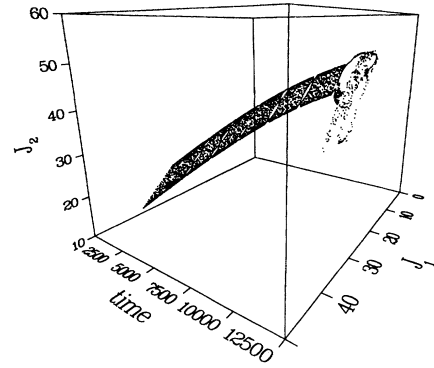We investigated, analytically and numerically, the dynamics of a two-dimensional Hamiltonian system whose parameters vary slowly in time. Our motivation was to study the dynamic autoresonance effect under conditions of a finite amount of energy in the driver.

We started with a specific model of two weakly interacting oscillators, one linear and the other nonlinear, with no explicit time dependence ("static" model). We studied the internal resonances in the system and transition to global chaos occurring for sufficiently large energies. Theoretical predictions made on the basis of the isolated-resonance approximation and Chirikov criterion of overlapping of the resonances were shown to agree well with the results of numerical simulations.

We generalized the well-known theory of internal resonances in two-dimensional Hamiltonian systems to the case of slowly varying parameters. In this case, the approximate integral of motion (38) was shown to hold, despite possible large changes of J_1 and J_2. We applied the theory to the "dynamic" version of the two weakly coupled oscillators' model and found the regime of DAR.

We suggested and verified numerically three constraints on the existence of DAR. The first of them is the same as in driven one-dimensional systems, and requires that the explicit time dependence of the parameters be slow compared to the nonlinear time scale of the corresponding static model. The second constraint is similar to that found in Refs. [8] and [10] for driven one-dimensional systems and is related to the transition to global chaos of the trajectories initially locked in DAR. The third constraint has no analogs in driven one-dimensional systems and involves the depletion of energy of one of the oscillators. Also, the bifurcation route for the time-dependent transition of the system from order to chaos was observed, as well as three qualitatively different routes for the inverse process.

ACKNOWLEDGMENTS

[1] L. D. Landau and E. M. Lifshitz, *Mechanics* (Pergamon, Oxford, 1976).

[2] D. Bohm and L. L. Foldy, Phys. Rev. **70**, 649 (1947).

[3] A. A. Kolomensky and A. N. Lebedev, *Theory of Cyclic Particle Accelerators* (North-Holland, Amsterdam, 1966).

[4] K. S. Golovanivsky, Fiz. Plazmy **11**, 295 (1985) [Sov. J. Plasma Phys. **11**, 171 (1985)].

[5] N. M. Kroll, P. L. Morton, and M. N. Rosenbluth, IEEE J. Quantum Electron. **QE-17**, 1436 (1981).

[6] B. Meerson, Phys. Lett. A **150**, 290 (1990).

[7] M. Deutsch, B. Meerson, and J. E. Golub, Phys. Fluids B **3**, 1773 (1991).

[8] B. Meerson and L. Friedland, Phys. Rev. A **41**, 5233 (1990).

[9] B. V. Chirikov, Phys. Rep. **52**, 263 (1979).

[10] B. Meerson and S. Yariv, Phys. Rev. A **44**, 3570 (1991).

[11] *Handbook of Mathematical Functions,* Natl. Bur. Stand. Appl. Math. Ser. No. 55, edited by M. Abramowitz and I. A. Stegun (U.S. GPO, Washington, DC, 1968).

[12] A. J. Lichtenberg and M. A. Lieberman, *Regular and Stochastic Motion* (Springer-Verlag, New York, 1983).

[13] V. I. Arnold and A. Avez, *Ergodic Problems of Classical Mechanics* (Benjamin, New York, 1968).